Smart Structures and Systems, *Vol. 24, No. 3 (2019) 361-377*
DOI: https://doi.org/10.12989/sss.2019.24.3.361

Modified sigmoid based model and experimental analysis of shape memory alloy spring as variable stiffness actuator

Bhagoji B. Sul[a] and K. Dhanalakshmi[*]

Department of Instrumentation and Control Engineering, National Institute of Technology, Tiruchirappalli, India

(Received August 7, 2018, Revised April 20, 2019, Accepted May 10, 2019)

Abstract. The stiffness of shape memory alloy (SMA) spring while in actuation is represented by an empirical model that is derived from the logistic differential equation. This model correlates the stiffness to the alloy temperature and the functionality of SMA spring as active variable stiffness actuator (VSA) is analyzed based on factors that are the input conditions (activation current, duty cycle and excitation frequency) and operating conditions (pre-stress and mechanical connection). The model parameters are estimated by adopting the nonlinear least square method, henceforth, the model is validated experimentally. The average correlation factor of 0.95 between the model response and experimental results validates the proposed model. In furtherance, the justification is augmented from the comparison with existing stiffness models (logistic curve model and polynomial model). The important distinction from several observations regarding the comparison of the model prediction with the experimental states that it is more superior, flexible and adaptable than the existing. The nature of stiffness variation in the SMA spring is assessed also from the Dynamic Mechanical Thermal Analysis (DMTA), which as well proves the proposal. This model advances the ability to use SMA integrated mechanism for enhanced variable stiffness actuation. The investigation proves that the stiffness of SMA spring may be altered under controlled conditions.

Keywords: shape memory alloy spring; helical tension spring; joule heating; variable stiffness actuation; nonlinear differential equation; experimental analysis; DMTA

1. Introduction

Reliable, accurate and efficient computational mathematical functions /models are essential for designing shape memory alloy (SMA) devices (He and Toi 2013). It is realized that the inherent stiffness varying property in the SMA material during actuation (its phase transformation) advances the ability of SMA to be integrated into suitable mechanisms that enhances the stiffness, thereby opportuning to variable stiffness actuation. The material stiffness of SMA plays a vital role in modelling the stiffness function of variable stiffness SMA actuator.

1.1 Background

1.1.1 Shape memory alloy

SMAs are typically metallic alloys that have the ability to recover a previously defined shape when subjected to an appropriate thermal procedure. Generally, these materials can be deformed at some relatively low temperature, and when heated they return to their shape prior to deformation. The shape recovery occurs even under applied loads therefore resulting in high actuation energy densities. The phase transformation causes the SMA to change its crystalline structure; SMA exist in two phases, the soft martensite (tetragonal, orthorhombic or monoclinic) occurs at the relatively lower temperatures and the stronger austenite (generally cubic) phase occurs at higher temperatures; their phase transformation is dependent on pre-stress and temperature. The phase transformation from martensite (product phase) to austenite (parent phase) and vice versa forms the basis for the unique behaviour of SMAs, the shape memory effect (SME) and pseudoelasticity (PE) (Lagoudas 2008). These important behaviour impact the response of dynamical systems configured with SMA and make SMA unique and appealing to be used in many scientific fields for actuation, sensing and in typical innovative engineering applications. The potential of shape memory effect is utilized to perform engineering functionalities like actuation (including self-sensing actuation (SSA), variable stiffness actuation (VSA)), to drive a mechanism / to do work, sensing, shared sensing and actuation, since the SMA when constrained generates force and provides displacement, in addition to exhibiting change in its electrical resistance, electrical inductance and elastic modulus; such of these can be exploited effectively in soft robots, assistive devices, automobile, automatic adjustment devices, aerospace, biomedical, home appliances and daily necessities, and so on. The mathematical representation/model describing the characteristics of SMA is a measure to explore its potential that fit to prospective applications (Jaronie Mohd Jani 2016). The force, displacement and stiffness in the phase transformation of SMA is affected by the input conditions (activation current, duty cycle and excitation frequency) and

*Corresponding author, Professor
E-mail: dhanlak@nitt.edu
[a] Ph.D. Scholar
E-mail: bbsul1975@gmail.com

http://www.techno-press.com/journals/sss&subpage=7 ISSN: 1738-1584 (Print), 1738-1991 (Online)

operating conditions (pre-stress and mechanical connection) (Zhang *et al.* 2013, Holanda et *al*. 2014, Wang *et al.* 2012, Raczka *et al.* 2011, Kumon *et al.* 2007, Liang and Rogers, 2003, Ikuta *et al*. 1991).

1.1.2 SMA as a variable stiffness actuator

Conventional actuators belong to the class of stiff / hard / rigid i.e., fixed stiffness actuators, while advancement in the actuation technology demanded the need for variable stiffness actuator; compliant / soft / flexible actuator belongs to the later class of actuators. A stiff actuator is a device that moves to a specific position or tracks a predefined trajectory. Once a position is reached, it will remain at that position, whatever the external forces exerted on the actuator (within the force limits of the device). A compliant actuator, on the other hand, will allow deviations from its equilibrium position (the position of the actuator where the actuator generates zero force or zero torque), depending on the applied external force. This concept is specifically introduced for compliant actuators, since it does not exist for stiff actuators. Variable stiffness actuators (VSAs) or adjustable compliant actuators are designed to be able to minimize the impact forces due to shocks, to safely interact with the user, and to store and release energy in passive elastic elements. It is preferred where safe human–machine interaction is required or in applications where energy efficiency must be increased by adapting the actuator’s resonance frequency (Van Ham *et al.* 2009). The shape memory alloy is a functional material; when it is joule heated, it has low (high) stiffness in the low (high) temperature martensite (austenite) phase; thereby exhibits material stiffness variation during the phase transformation. The SMA spring can change it stiffness by three to four times during actuation (Liang and Rogers 1997). The stiffness of SMA spring is linearly related to its elastic modulus. An alternative is to integrate mechanisms into a structure and change the stiffness by altering boundary conditions and structural load paths.

1.2 Previous work on modelling the stiffness of SMA

Ikuta is the pioneer in introducing about stiffness of SMA directly for feedback control in 1990. Since the stiffness of SMA can be considered corresponding to phase transformation directly, the stiffness of SMA can be directly known by using its electric resistance (Ikuta 1990). Since then, the stiffness of SMA is explored to be utilized for feedback control and variable stiffness application. Thereby the phase transformation (SME) of SMA for (variable stiffness) actuation is modelled by involving its stiffness and has been presented broadly by the different constitutive models, which are polynomial and linear (Raczka *et al*. 2011, Kumon *et al.* 2007, Ikuta 1990, Liang and Rogers 1997, Bendane 2010), exponential (Holanda *et al*. 2014) and trigonometric (Raczka *et al*. 2011) in nature. Double-supported SMA bar that work like SMA spring is used in the synthesis and analysis of controlled vibration reduction systems, in which, the model takes into account the relationship of stiffness and damping to alloy temperature and the frequency of excitation (Raczka *et al*. 2011). The stiffness of SMA helical spring actuator is represented as a linear model by relating to its normalized resistance, to be applicable for stiffness control (Kumon *et al.* 2007 and Ikuta 1990). According to Liang and Roger (1997), the shear modulus and stiffness of SMA spring varies with its temperature while the nature of curve relating the stiffness of SMA spring and its surface temperature is “S” shape. The phase transformation of SMA helical spring actuator is modelled as a logistic function of temperature during heating and cooling (Ikuta *et al*. 1991); and the complex stiffness of SMA helical spring actuator is modelled using the above functions for vibration control (Holanda *et al*. 2014). It is presented that the spring stiffness has nonlinear behaviour and it changes with force at constant displacement; the model uses the tan hyperbolic function (Raczka *et al*. 2011). The dynamic mechanical analysis of NiTi reveals the nature of storage modulus, loss modulus and damping with respect to time, frequency, strain and temperature (Da Silva *et al*. 2009). Review on the concept of variable stiffness actuators and compliant actuator design are presented respectively (Sabastian *et al*. 2016, Van Ham *et al*. 2009). These models exhibit limitations and hence this paper focuses to provide a new model for the material stiffness of the phase transformation in SMA helical spring.

The phase transformation of SMA depends on temperature / current, pre-stress and frequency, which rely on the material properties like specific heat, density, volume / area and convective heat transfer coefficient. The phase transformation can be modelled for force, pre-stress, displacement, also for stiffness with respect to input thermal / electrical power.

The accuracy of the model in polynomial form is dependent on its order. In general, the truncated function or a linear function is used to simplify the representation; this propagates the error since the order is reduced/less. Furthermore, it presents an incomplete mathematical mapping of the respective functional variable since the linear portion of operation is alone considered (Raczka *et al*. 2011, Kumon *et al*. 2007 and Liang and Roger 1997). The models are unable to explain their effect on stiffness, without involving important factors like pre-stress or load (as constant or variable) (Raczka *et al.* 2011) and frequency. Though mapping in terms of force, stiffness, displacement, pre-stress or electrical resistance is modelled by logistic function (Bhagoji and Dhanalakshmi 2017, Ikuta 1990, Holanda *et al*. 2014, Zhang *et al*. 2013, Cortez-Vega *et al*. 2018, Sibielak *et al*. 2016, He and Toi 2013), they have failed to involve the factors like frequency, temperature, duty cycle, and pre-stress which decide the phase transformation/hysteresis characteristics.

1.3 Present work on modelling the stiffness of SMA spring actuator

The possibilities of modelling the phase transformation characteristics i.e., functional variables of SMA as actuator is pictorially presented in Fig. 1; also indicating (highlighted) the direction of the present work. This work

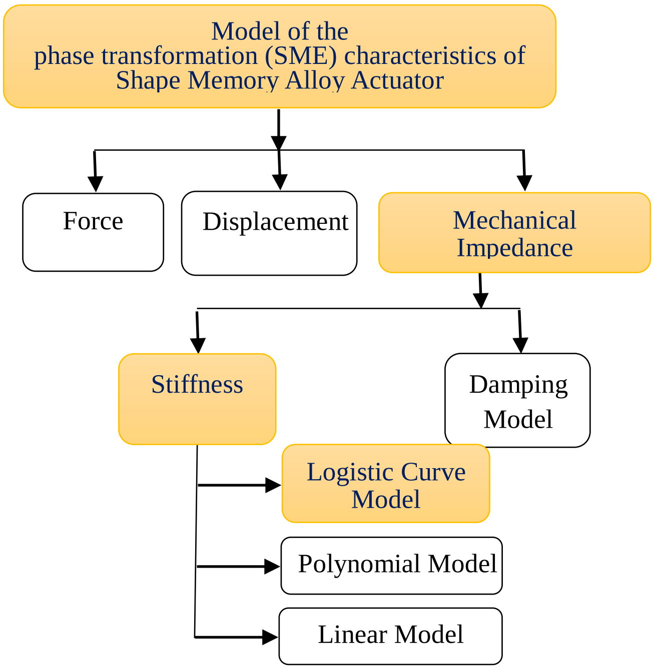

Fig. 1 Representation of the functional variables of actuation of SMA, models and types

aims to eliminate the limitations of the previous models to represent the stiffness i.e., to represent a simple, complete functional mapping of SMA spring stiffness, to involve the important factors of phase transformation/hysteresis characteristics (frequency, temperature / current, duty cycle and pre-stress) and most importantly, include the effect of Joule heating. This can further lead to obtain the mathematical representation of stiffness of an SMA spring integrated and actuated configuration / mechanism, for an application to adapt with dynamic environments. The best part is that there is a scope to represent the electro-thermo-mechanical model of the actuation (and variable stiffness actuation) of SMA (unlike the earlier models which are mostly only thermo – mechanical in nature) since the Joule heating of SMA facilitates the success of control. The conventional phenomenological models, like the exponential function model and cosine function model are fixed shape transformation hardening functions which are incapable to represent the behaviour of SMA accurately; hence, there is considerable scope for improving the existing models explained (He and Toi 2013).

This work proposes an empirical model that is derived from the logistic differential equation to completely model the stiffness of SMA spring actuator by considering the important factors current, frequency, duty cycle and pre-stress, thereby and, enables to capture the flexible shape recovery behaviour since the sigmoid function has the flexibility to adjust for its smooth curve shape by using rate coefficient. The model is validated through simulation and experimentation.

Objectives of the work

- To obtain an empirical model of the stiffness of SMA tension spring that is derived from the logistic differential equation, thereby relate the model of the SMA spring actuator in the passive antagonistic configuration.
- To analyse the effect of activation current, frequency, duty cycle and pre-stress on the temperature dependent stiffness.
- To validate the empirical model through experimentation and compare with reported models on stiffness.

Outline and Technical uniqueness of the work

- An empirical model of the stiffness of SMA spring is proposed which is more adaptable and a better fit to the typical SMA stiffness - temperature relationship.
- This model overcomes the short comings of the existing models which has fixed shape transformation hardening functions and may not be able to represent the behaviour of polycrystalline SMA (since the transformation speed always change).
- The proposed model is validated experimentally and also compared with the previously reported polynomial model and logistic curve model of stiffness.
- Parameter estimation is performed offline by nonlinear least square method
- The stiffness of SMA is explored under different current, frequency, duty cycle and pre-stress.
- The overall stiffness of the actuator configured with SMA spring and parallel steel tension bias spring increases qualitatively but decreases quantitatively with increase in the stiffness of SMA

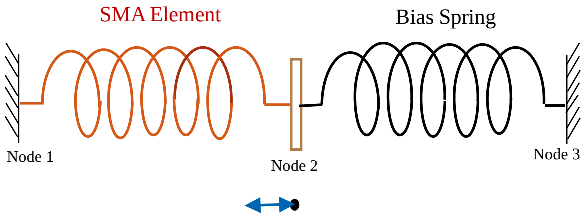

Fig. 2 Passive bias variable stiffness SMA actuator

spring, thereby functioning as an active variable stiffness actuator (it is therefore compliant in nature).

- The nature of stiffness variation in the SMA spring is assessed also from the Dynamic Mechanical Thermal Analysis (DMTA) which verifies the nature of the model; further, supports the understanding about the nature of stiffness variation and influence of current, frequency, duty cycle and pre-stress.

2. Variable stiffness actuator using SMA spring

The SMA spring by its physical phenomenon, characteristically possess the stiffness variation. The objective is to model i.e., mathematically represent the actuation function of SMA spring, in terms of its stiffness. To enable repetitive actuation, the SMA spring is to be arranged along with a passive bias element such that the combination is flexible / compliant which does not alter / affect the stiffness in the SMA element. A passive antagonistic arrangement (the SMA element and the bias element always acts against each other) / series connection is preferable due to its compactness, simplicity, effectiveness and being lightweight. An individual one way actuating SMA element cannot function as an actuator, a bias element is required in a suitable combination to function cyclic; this leads to a fundamental biased configuration of SMA actuator. The (one-way Shape Memory Effect) SMA spring can contract only in one direction about the equilibrium; a bias force (recovery force of passive spring or pre-stress spring) is necessary to return the SMA in its neutral position. The passive bias type active variable stiffness actuator is shown in Fig. 2. The mode of operation is work production or actuator and generates stress when (joule) heated.

The stiffness variation in the SMA spring is realized by changing the electrical power of Joule heating, driving frequency and pre-stress by simultaneous change in force and displacement of SMA spring. This configuration changes the overall stiffness as the SMA spring stiffness increases and decreases during heating and cooling cycle due to joule heating; therefore, the overall configuration's stiffness changes.

3. Proposed modification of the sigmoid based model of the stiffness of SMA spring actuator

It is essential to know the mechanical properties of SMA (stiffness, damping, force, displacement, stress, strain), to employ it in the design of applications that are characterized by shock absorption, adaptive to unknown environments and gentle interaction (e.g., soft robotics, human assistive devices, medical surgical devices). There are strong relationships of the mechanical properties of SMA spring with driving frequency, temperature and external pre-stress.

It is advisable to represent and relate them mathematically, to be used in the control law. SMA element can be considered as a three-element system in which electrical energy is converted into thermal energy and then to mechanical work. Despite their quality, most of the models available in literature are difficult to be used in practice: they are quite complex mathematical equations that require burdensome numerical solution. This section discusses the key factors (thermal behavior and nature of force) associated with the dynamic stiffness of SMA, suitable for easy analytical prediction.

3.1 Mathematical representation of force and displacement of the SMA spring actuator

Restraining the deformed SMA while heating above its phase transition temperature will generate a large. The real-world phase transformation behavior of SMA does not strictly follow a fixed path; also the transformation speed will not always remain the same because of its polycrystalline structure. But most of the conventional models represent the fixed shape transformation hardening functions; hence, are incapable of representing the true nature of phase transformation. To overcome the shortcomings of existing models, this research proposes the sigmoid function to afford a better fit to the typical SMA force and temperature, displacement and temperature and, stiffness and temperature relationships. A more flexible function, the sigmoid function has been introduced for representing the phase transformation.

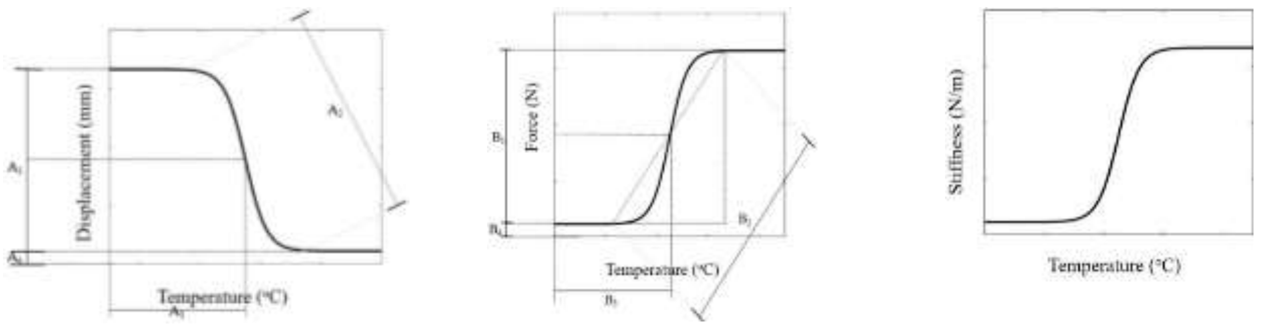

(a) (b) (c)

Fig. 3 The nature of variation of force, displacement and stiffness in SMA spring actuator

The sigmoid function has a flexibility to adjust its curve shape by using four functional parameters, which differs during heating and cooling, with change in temperature, frequency and pre-stress. The phase transformation rate coefficient, which is one of the functional parameter is used to represent the transition speed of the phase transformation. It is also able to describe the slow and gradual phase transformation in the starting and finishing regions of the entire phase transformation. Thereby, it enhances the flexibility as well as ensures the consistence of martensitic phase fraction (He and Toi 2013). The width of the hysteresis depends on the driving frequency and external pre-stress. The functional parameters change simultaneously with the driving frequency and pre-stress (Zhang *et al.* 2013).

The application is designed using SMA in three different ways 1) free recovery mode in which the sole function of the memory element is to cause motion or strain on the applications.2) Constrained recovery mode in which the memory element is prevented from changing shape and thereby generates a stress or force on the applications. 3) Work production mode in which there is motion against a pre-stress and thus work is being done by the memory element on the application. It can be one way or two way SMA.

In the literature, the phase transformation is explained dominantly by the hysteresis characteristics that relates stress – strain (Da Silva *et al*. 2009 and He and Toi 2013), force – displacement (Raczka *et al*. 2011 and Kardan *et al*. 2013), displacement and voltage (Zhang *et al.* 2013), electric resistance and temperature (Kumon *et al*. 2007), force and temperature (Raczka *et al*. 2011), (Bhagoji and Dhanalakshmi 2017) and (Cortez-Vega *et al*. 2018), stiffness and temperature, elastic modulus and temperature (Holanda *et al*. 2014), displacement and current (Marek *et al.* 2016) which are represented from different governing laws and, they dominantly exhibit the ‘S’ shape characteristic for the heating and cooling cycles; these cycles together form the hysteresis. Thereby, the force is function of temperature during the heating and/or cooling cycle of the SMA spring is represented by sigmoid function as shown in Fig. 3(b).

The nature of the phase transformation characteristic of SMA spring that relates force and temperature matches (goes in hand) with the logistic differential equation (nonlinear ordinary differential equation) mathematically

$$\frac{dF}{dT} = B_2*(1-\frac{F}{B_1}) \tag{1}$$

where, F is force generated by SMA spring (N) due to Joule heating, T is temperature of SMA spring (^oC), B_1 is the maximum value of force generated by SMA spring (N) and B_2 is the rate of force with respect to temperature of SMA spring (N/^oC). The solution of Eq. (1) is a sigmoid function

$$F = B_4 + \frac{B_1}{1+EXP(-B_2*(T-B_3))} \tag{2}$$

where, B_3 is the initial temperature (^oC) and B_4 is initial force (N). It is evident that the sigmoid function is bounded by two asymptotic lines: F = B_4 is the lower value of asymptotic line, F = B_1 is the upper value of asymptotic line. Eq. (2) is depicted in Fig. 3(b) and relates for work production mode of operation of SMA when both force and displacement are varying. Eq. (2) is applicable during both the phases of heating as well as cooling to determine the force.

Similarly, the displacement or change in length of SMA spring due to Joule effect in terms of temperature is understandable and approximated by the logistic differential equation (nonlinear ordinary differential equation) as

$$\frac{dX}{dT} = A_2*(1-\frac{X}{A_1}) \tag{3}$$

where, X is the displacement of SMA spring (m) due to Joule heating, T is temperature of SMA spring (^oC), A_1 is the maximum value of displacement of SMA spring (m) and A_2 is the rate of displacement with respect to temperature of SMA spring (m/^oC). The solution of Eq. (3) is a sigmoid function

$$X = A_4 + \frac{A_1}{1+EXP(-A_2*(T-A_3))} \tag{4}$$

where, A_3 is the initial temperature of the SMA spring (^oC) and A_4 is the initial displacement (m). It is evident that the sigmoid function is bounded by the two asymptotic lines: X = $A_3$is the lower value of asymptotic line and, X = A_1 is the upper value of the asymptotic line. Eq. (4) is depicted

Fig. 4 Mechanical arrangement of the SMA spring actuation system

in Fig. 3(a) which relates for variation of both force and displacement of SMA spring during work production mode.

3.2 Mathematical representation of stiffness of SMA spring actuator

The stiffness of SMA plays an important role in applications employing variable stiffness actuators, to provide smart way to use (store and release) the energy.

The important aspects of such actuators are safety, robustness and dynamic performance like in human – machine interaction (HMI) systems and applications. In these systems, the joint stiffness can be changed by virtue of material property, mechanically in the variable stiffness actuator and/or by the controller.

The contraction force of the SMA spring is not constant, rather changes with the shear (Young's) modulus. The spring constant/stiffness of an SMA spring, as a linear function of its shear (Young's) modulus, increases 3 to 4 times within the phase transformation temperature range for the heating process. During cooling, the contraction force in turns of the stiffness of the SMA spring decreases with shear modulus which varies with temperature due to the material property (Liang and Rogers 1997). The nonlinear stiffness of nonlinear SMA spring is mathematically represented by Dr. Ben.

$$K_1 = \frac{dF}{dX} \tag{5}$$

where, stiffness is the change in force with respect to change in displacement. From which

$$K_1 = \frac{dF}{dX} = \frac{dF}{dT} \times \frac{dT}{dX} \tag{6}$$

Using Eqs. (2) and (4) in Eq. (6) leads to

$$K_1 = \frac{B_1 * B_2 * EXP(-B_2*(T-B_3)) * (1+EXP(-A_2*(T-A_3)))^2}{A_1 * A_2 * EXP(-A_2*(T-A_3)) * (1+EXP(-B_2*(T-B_3)))^2} \tag{7}$$

where, A_1, A_2, A_3, B_1, B_2 and B_3 are parametric constants which depend on driving frequency, pre stress, current and duty cycle. The stiffness is represented by different sigmoid functions which present similar behaviour but are related by different parametric constants, for the heating and cooling cycles.

Therefore, the stiffness to temperature characteristic(s) shown in Fig. 3(c) also is in 'S' shape or a representation of sigmoid curve(s), since its nature is the same as that of force to temperature, indicating that the SMA spring stiffness has nonlinear behaviour.

3.3 Stiffness of the SMA spring with antagonistic passive bias spring configuration for actuation

In the passive bias antagonistic configuration of series SMA spring actuator, as shown in Fig. 4, the SMA spring is nonlinear and possess nonlinear stiffness K_1 in N/m; while the passive bias steel possess constant stiffness K_2 in N/m.

The overall stiffness of the passive bias antagonistic configuration of parallel SMA spring actuator is

$$K = K_1 - K_2 \tag{8}$$

where K_1 is the stiffness of SMA spring (N/m) and K_2 is the stiffness of the steel spring (N/m).

The net stiffness of the configuration i.e., the overall stiffness of the actuator is less but it increases with increase in stiffness of SMA spring; therefore, the passive bias antagonistic configuration of parallel SMA spring actuator is variable in nature.

4. Parameter estimation of the stiffness model of the SMA spring actuator

To validate the model experimentally, it is necessary to find out/determine the parameters of the derived model. The data from the experiments are used in the nonlinear least square method of parameter estimation to attain the response of the model.

4.1 Laboratory test facility

The experimental test facility is designed and fabricated as shown in Fig. 5, to experimentally estimate the model parameters of stiffness of SMA spring actuator; thereby experimentally validate the proposed model. The experimental set up has three major hardware sections:

1) The basic SMA spring actuation system which consists of a mechanical arrangement to configure the mechanically parallel connection of SMA tension spring with variable stiffness k_1 with its passive bias steel tension spring with constant stiffness k_2 for antagonistic operation. The mechanical support system includes the fixed frame to which are attached guide rods along with linear bearings on both/either sides of the SMA spring actuator to enable uniform and continuous hurdle-free movement. A flap in between the springs aids the measurement of displacement of SMA spring.

Fig. 5 Experimental facility for parameter estimation and model validation

Table 1 Technical specifications of SMA spring (Flexinol®)

Properties	**Range / Value**
Physical properties	
Melting point	1310 ℃
Electrical resistivity	76 x10^{-5} ohm-m
Modulus of elasticity	28 – 41 GPa
Latent heat of transformation	5.78 kCal/kg
Thermal conductivity	18.0 W/m℃
Thermal expansion coefficient	Martensite 6.6x10^{-6} /℃ Austenite 11.0 x 10^{-6} /℃
Poisson ratio	0.33
Electrical resistivity	Martensite 80 x10^{-8} ohm-cm Austenite 100 x10^{-8} ohm-cm
Specific heat, C_p	1.84 J or 0.44 kCal/kg °C
Convective heat transfer coefficient, h	54.50
Transformation temperature	
Ingot austenite finish (A_f)	75 to 110℃
Finished product A_f	50 to 80℃
Mechanical properties	
Ultimate tensile strength	≥ 1070 MPa
Total elongation	≥ 10%
Loading plateau stress @ 3%	≥ 100 MPa
Shape memory strain	≤ 8.0%
Geometrical parameters	
Wire diameter	5.0x10^{-4} m
No. of coils	45
Coil diameter	3.0x10^{-3} m
Volume	81.67x10^{-8} m^2

2) A comparator (IC 324) with MOSFET (TIP 122) circuit is designed to drive and control the SMA actuation system.
3) The instrumentation system includes a miniature load cell (nonlinearity of +/- 0.25 % of full scale) mechanically in series with the SMA spring placed at the fixed end, a laser displacement sensor (Keyence made) focusing on the movable end of the SMA spring (on the flap) and J type micro thermocouple (Omega made super MCJ with 1 mV/

Table 2 Technical specifications of stainless steel spring

Physical properties (EN42J)	**Value**
Hardness	220 HV max
Yield stress	290 MN/m^2 min
Tensile strength	640 MN/m^2
Spring rate(Stiffness constant)	130 N/m

Table 3 Estimated parameters of the stiffness model at 10 mHz under different currents

Parameters / Current (A)	A_1	A_2	A_3	B_1	B_2	B_3
HEATING CYCLE PARAMETERS						
1.0	0.7226	4.5500	2.0000	0.5411	4.769	2.5380
1.5	0.7870	2.4730	2.4900	0.6307	2.6761	3.0040
2.0	0.9778	1.1350	2.7540	1.0730	1.0940	3.7330
COOLING CYCLE PARAMETERS						
1.0	0.6515	23.2500	2.7090	0.5031	23.7700	2.7210
1.5	1.2250	1.8290	2.0730	0.9400	2.0660	2.5280
2.0	0.4069	2.6930	2.2230	0.4126	2.4880	2.6490

Table 4 Estimated parameters of the stiffness model at 10 mHz under different loads

Parameters / Load (g)	A_1	A_2	A_3	B_1	B_2	B_3
HEATING CYCLE PARAMETERS						
100	0.6590	3.0290	3.390	0.5196	3.2510	3.5260
150	0.7096	2.1240	3.1430	0.6893	2.2130	3.5590
200	0.3156	2.0740	2.5720	0.3409	1.9810	3.1600
COOLING CYCLE PARAMETERS						
100	0.9557	2.0950	3.4870	0.7279	2.2940	3.6950
150	1.3810	1.4950	3.5890	1.3070	1.5740	4.1420
200	0.6976	1.8010	3.0450	0.7277	1.8040	3.6190

^{o}C or 1 mV/ ^{o}F sensitivity) placed at the center of the SMA spring; a current transducer is connected electrically in series with the SMA spring. All the data (the force, displacement, temperature and current in the range of 0 to 10 V) are recorded and transferred to a PC via a data acquisition system (MCC DAQ card 1408FS plus).

The technical specifications of SMA spring and steel spring are presented in Tables 1 and 2 respectively. The bias spring allow smooth deflection of the SMA spring during activation and deactivation. When the NiTi spring is electrically heated, it undergoes a phase transformation to the stronger austenite. Once the electric current is reduced to zero, the SMA spring cools and transform back to the weaker martensitic phase.

4.2 Experimentation

A series of experiments is conducted to determine the parameters of the stiffness model and validate its response experimentally, at different conditions like activation current, driving frequency and pre-stress, for work production or actuator mode (for force and deflection varying simultaneously).

The sine wave input to the comparator generates a square wave at different pulse width in accordance to the input sinusoidal frequency, which will act as the input to the MOSFET (switch) of the current amplifier, to drive the SMA spring in a controlled manner.

Table 5 Estimated parameters of the stiffness model at 2 A under different frequencies

Parameters / Frequency (mHz)	A_1	A_2	A_3	B_1	B_2	B_3
HEATING CYCLE PARAMETERS						
10	0.4415	2.9600	2.7100	0.3995	3.0550	2.9520
30	0.4187	10.0800	3.0550	0.4096	10.4900	3.0920
50	0.2222	5.7580	2.2850	0.2107	5.8630	2.4340
COOLING CYCLE PARAMETERS						
10	0.8171	1.2270	2.9350	0.7851	1.2280	3.7020
30	0.3599	2.1780	2.7650	0.3578	2.2530	3.1750
50	1.4930	2.9890	2.5090	1.4170	3.2350	2.7540

Table 6 Statistical analysis of nonlinear least square method under different currents

Current / Statistical Parameters	1.0		1.5		2.0	
	Heating Cycle	Cooling Cycle	Heating Cycle	Cooling Cycle	Heating Cycle	Cooling Cycle
Sum Squared Error (SSE)	0.0536	0.0087	0.0118	0.0159	0.0059	0.0073
R-Squared Value	0.9980	0.9973	0.9980	0.9987	0.9980	0.9978
Root Mean Squared Error	0.0251	0.0103	0.0133	0.0114	0.0164	0.0108
Adjusted R- Squared Value	0.9880	0.9973	0.9979	0.9986	0.9976	0.9986

The possible three modes of operation of SMA spring as an actuator are

1) Variable displacement at constant force (Free recovery) 2) Variable force at constant displacement (Constraint recovery) 3) Simultaneous variation of force and displacement (Work production). The most practical and applicable mode of operation is work production. In mode 1 and 2, the stiffness is direct function of displacement and the force respectively; the model of stiffness is the model of displacement and force. The controllable actuator is derived from the mode 3 which is favourable in nearly all practical engineering applications where force and deflection vary simultaneously. The free recovery or variable deflection mode is used in Simon inferior vena cava (IVC) filter and eyeglass frames. The constrained recovery or variable force mode finds application in hydraulic coupling, fasteners and connectors. Few applications of mode 3, the actuator or work production mode, where both force and deflection changes are circuit breakers and heat engines etc.

4.3 Parameter Identification of the Model

The SMA spring is a nonlinear element and it displays hysteresis among different actuation variables, it is true with stiffness also; all the hysteresis curves of SMA spring actuator are sigmoid-like. Referring to the proposed model of stiffness for the variable stiffness actuation of SMA spring presented in Eq. (7), the parameters are identified offline from the experimental data. From Eq. (7), it is understood that the stiffness is affected by temperature/current, pre-stress/load and driving frequency simultaneously. Therefore, these three factors are considered separately for simplicity, to understand their individual effect on the stiffness. The experimental data are employed through nonlinear least square approximation to identify/estimate the parameters of the hysteresis profiles of stiffness; the parameter values are listed separately in Tables 3-5 respectively, corresponding to the different currents, stresses and sinusoidal frequencies. It is not intended to find the general parameters of the model for all conditions rather can be used for suitable applications.

5. Model validation

The model is validated by considering the correspondence between the SMA spring actuator dynamics and experimental information. Also, the statistical analysis of the nonlinear least square method is acquired. The simulation results (model response) predicted by the modified sigmoid based model are shown in Figs. 6-8 in comparison with the experimental response for different currents, stresses/loads and frequencies respectively.

The four important parameters of statistical analysis of the model response through nonlinear least square / regression method that signify the performance are 1) Sum Squared Error (SSE) 2) R-Squared 3) Adjusted R-Squared and 4) Root Mean Squared Error.

Table 7 Statistical analysis of nonlinear least square method under different stresses

Load / Statistical Parameters	100 g		150 g		200 g	
	Heating Cycle	Cooling Cycle	Heating Cycle	Heating Cycle	Cooling Cycle	Heating Cycle
Sum Squared Error (SSE)	0.0016	0.0023	0.0580	0.0016	0.0023	0.0580
R-Squared Value	0.9992	0.9989	0.9982	0.9992	0.9989	0.9982
Root Mean Squared Error	0.0089	0.0095	0.0175	0.0089	0.0095	0.0175
Adjusted R Squared Value	0.9990	0.9987	0.9977	0.9990	0.9987	0.9977

Table 8 Statistical analysis of nonlinear least square method under different frequencies

Frequency / Statistical Parameters	10 mHz		30 mHz		50 mHz	
	Heating Cycle	Cooling Cycle	Heating Cycle	Heating Cycle	Cooling Cycle	Heating Cycle
Sum Squared Error (SSE)	0.0067	0.0041	0.0218	0.0067	0.0041	0.0218
R-Squared Value	0.9986	0.9981	0.9950	0.9986	0.9981	0.9950
Root Mean Squared Error	0.0138	0.0065	0.0289	0.0138	0.0065	0.0289
Adjusted R- Squared Value	0.9984	0.9980	0.9940	0.9984	0.9980	0.9940

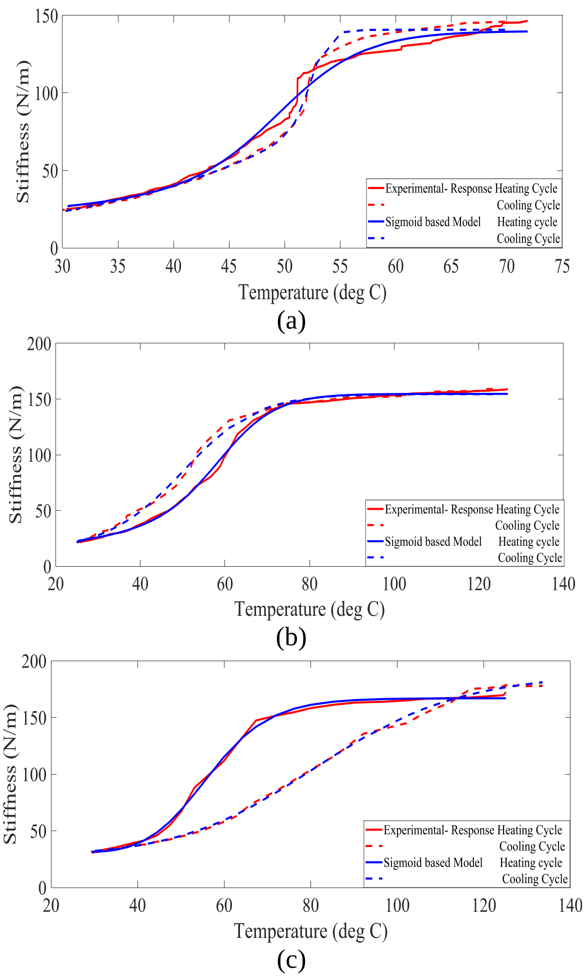

Fig. 6 Theoretical and experimental stiffness profiles of SMA spring for temperature sweep at 10 mHz for (a) 1 A, (b) 1.5 A and (c) 2 A

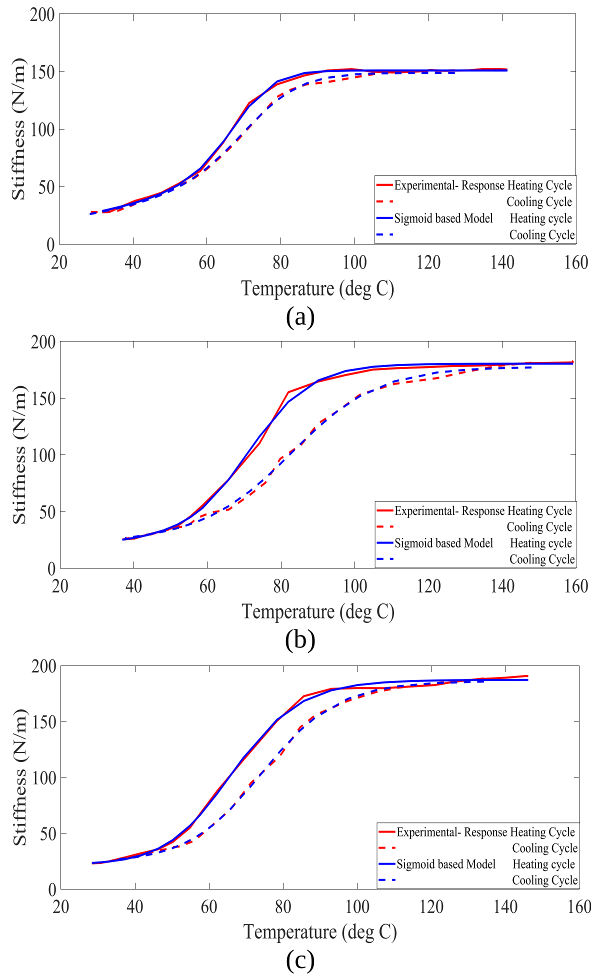

Fig. 7 Theoretical and experimental stiffness profiles of SMA spring for temperature sweep at 10 mHz for (a) 100 g, (b) 150 g and (c) 200 g

The numerical values of these errors are presented in Tables 6-8 accordingly, which indicates that the root mean square errors (RMSE) are near zero and the R-squared values are nearly equal to one, thereby indicating a higher correlation factor, indicating absolute fit and greater portion of variance is accounted by the model. The quality of approximation or fitting of the model improves at current or temperature and stress within the range of specifications of SMA spring.

6. Comparison with other models

The significance of the proposed modification is evaluated by comparing with two different models proposed in the literature.

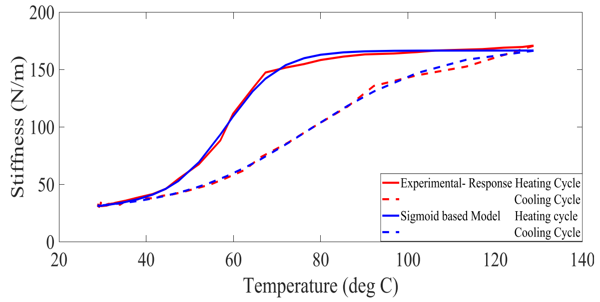

(a)

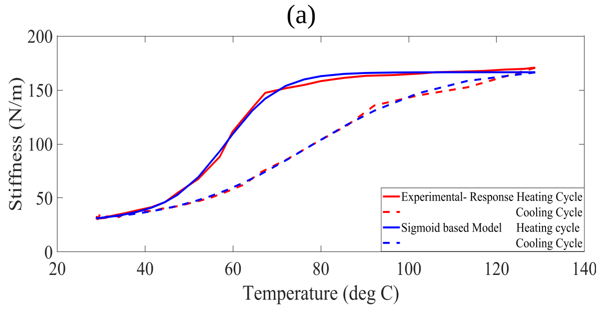

(b)

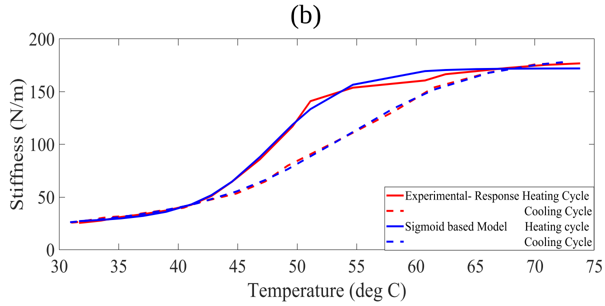

(c)

Fig. 8 (a) Theoretical and experimental stiffness profiles of SMA spring for temperature sweep at 2 A for 10 mHz, (b)Theoretical and experimental stiffness profiles of SMA spring for temperature sweep at 2 A for 30 mHz and (c) Theoretical and experimental stiffness profiles of SMA spring for temperature sweep at 2 A for 50 mHz

6.1 Logistic curve model

The proposed stiffness model is compared with the simplified mathematical model of stiffness presented as a function of temperature of the SMA spring (Holanda *et al*. 2014). Eqs. (9) and (10) are used to simulate the responses during heating and cooling for the experimentally collected data.

$$K_A=K_{min}+(K_{max}-K_{min})-\frac{K_{max}-K_{min}}{1+EXP\left(\left(\frac{6.2}{A_f-A_s}\right)*\left(T-\frac{A_s-A_f}{2}\right)\right)} \quad (9)$$

where $K_A(K_M)$ is the stiffness during heating (cooling), K_{min} (K_{max}) is minimum (maximum) stiffness, $M_s(M_f)$ is martensite start (finish) temperature, $A_s(A_f)$ is austenite start (finish) temperature and T is the temperature, of the SMA spring. The stiffnesses are in N/m and temperatures are in ^oC.

The values used in the model (Eqs. 9 and 10) are: The transformation temperatures of the SMA spring (M_s= 61.48 ^oC, M_f = 58.72^oC, A_s= 73.83^oC and A_f = 80.4^oC) obtained from the Differential Scanning Calorimeter (DSC) Test. The minimum and maximum values of stiffness, K_{min} and K_{max} used from the experimental information, corresponding to the conditions of analyses as shown in Figs. 9-11, which are the stiffness profiles of comparison, are respectively 21.78 N/m and 159.07 N/m, 30.71 N/m and 169.58 N/m and, 34.78 N/m and 153.97 N/m.

$$K_M=K_{min}+(K_{max}-K_{min})-\frac{K_{max}-K_{min}}{1+EXP\left(\left(\frac{6.2}{M_s-M_f}\right)*\left(T-\frac{M_s+M_f}{2}\right)\right)} \quad (10)$$

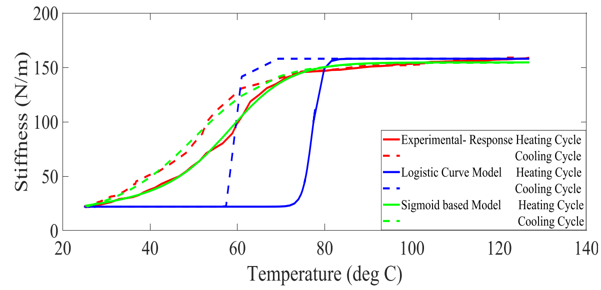

Fig. 9 Stiffness profiles of experimentation, Logistic curve model and the Modified Sigmoid based model of SMA spring at 10 mHz, 1.5 A

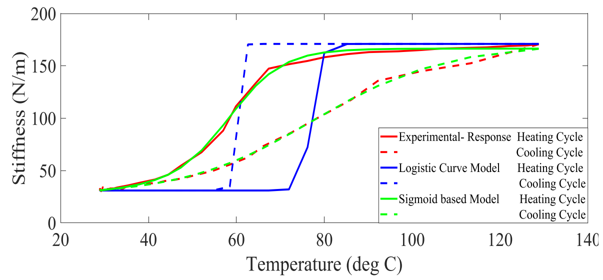

Fig. 10 Stiffness profiles from experimentation, the Logistic curve model and the Modified Sigmoid based model of SMA spring at 2 A,10 mHz

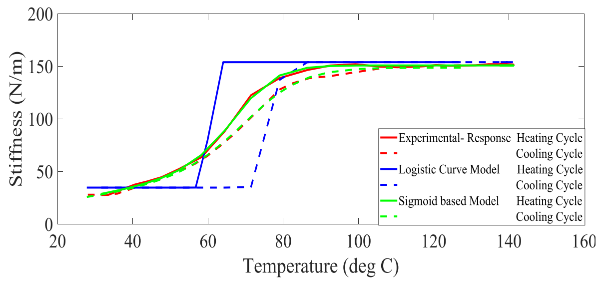

Fig. 11 Stiffness profiles from experimentation, the Logistic curve model and Modified Sigmoid based model of SMA spring at 100 g, 10 mHz and 2A

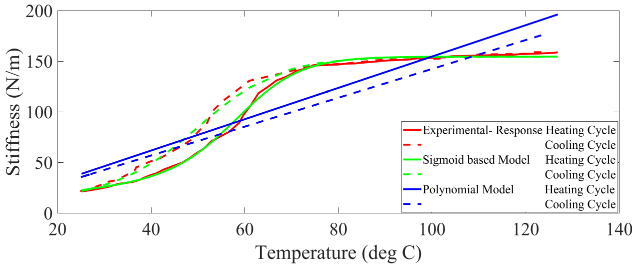

Fig. 12 The stiffness profiles of SMA spring from experimentation, the Polynomial model and the Modified Sigmoid based model at 10 mHz for 1.5 A

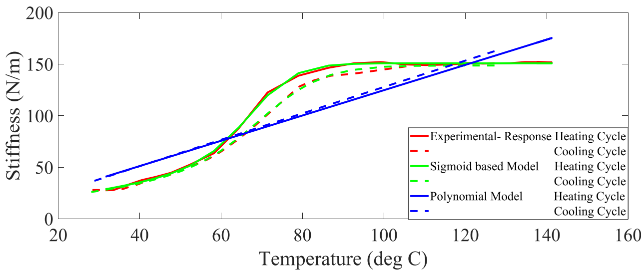

Fig. 13 The stiffness profiles from experimentation, the Polynomial model and Modified sigmoid based model at 10 mHz, 2 A for 100 g

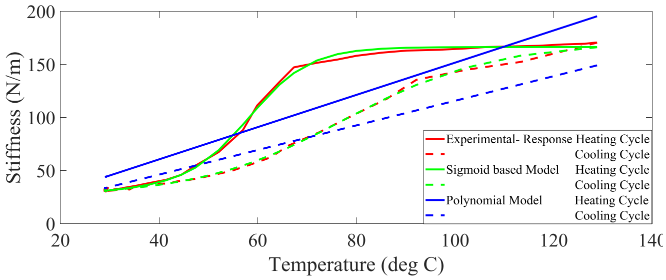

Fig. 14 The stiffness profiles from experimentation, the Polynomial model and Modified sigmoid based model at 2A for 10 mHz

Though the model tries to capture the dynamics of the original information i.e., experimental data, it is not smooth but appears as straight lines with abrupt changes. Anyhow, the effect of current, stress and frequency is observed on the stiffness hysteresis band and its minimum and maximum levels.

6.2 Polynomial model

The spring rate K of a spring comprised of double supported SMA bar (Raczka *et al.* 2011) is explained using the mathematical model.

$$K=a_1+a_2*f+a_3*f^2+a_4*T \tag{11}$$

where a_1, a_2, a_3 and a_4 are determined using the nonlinear least square method. f is the frequency of excitation in mHz and T is the temperature in ^{o}C; these parameters are different for different currents, stresses and frequencies. The respective values are used to plot the model response in comparison with the response of the sigmoid based model and referenced to the experimental response, as shown in Figs. 12-14. The polynomial model and the modified sigmoid based model of stiffness profiles convey comparison and say that the polynomial model is unable to capture the original dynamics like that of the modified sigmoid based model. Also, the effects of current, stress and frequency are observed on the stiffness hysteresis band and its minimum and maximum levels, but is very minimal and poor since it does not capture the nature at all.

7. Experimental analysis of stiffness of shape memory alloy spring actuator

7.1 Electro-thermo-mechanical behaviour of SMA spring actuator

The change in the Young's modulus of SMA is different in nature from most conventional metallic materials, such that in metals it decreases with increase in temperature whereas in SMA it increases during the heating process of the phase transformation. Also during heating above transition temperature, SMA will generate large reaction force and recover its parent shape. The same nature is followed by shear modulus and stiffness of SMA spring. Such distinctive characteristics of SMA are exploited in many applications as actuators.

The electro-thermo-mechanical characteristics of SMA spring actuator in work production mode i.e., under simultaneous variation of force and displacement are expedited experimentally, and presented in Figs 15-18 to evaluate the effect of current, pre-stress, driving frequency and duty cycle respectively. These static characteristics represent the relationship of spring reaction force to its deflection. The experimentation is carried out to explore the behavior within its rated specifications/capacity; the ranges of current, pre-stress and frequency of excitation and duty cycle are 0 to 2 A, 0 to 75 MPa, 0 to 50 mHz and 20 to 80 % respectively.

7.1.1 The effect of current

The effect of current is determined only for the heating cycle, since work (actuation) is done only then. The electrical current heats the SMA spring; thereby, the effect of temperature due to change in current is obtained on the

Table 9 Effect of current on temperature and stiffness at 10 mHz

Properties / Current (A)	Temperature (°C)		Stiffness (N/m)	
	Minimum	Maximum	Minimum	Maximum
1.0	30.08	71.87	24.39	146.54
1.5	25.01	123.04	21.78	159.07
2.0	29.22	130.77	29.96	180.26

Table 10 Effect of stress/load on temperature and stiffness at 10 mHz

Properties / Load (g)	Temperature (°C)		Stiffness (N/m)	
	Minimum	Maximum	Minimum	Maximum
100	35.5	141.25	34.78	153.97
150	36.73	159.21	25.38	184.99
200	27.24	146.20	23.16	189.52

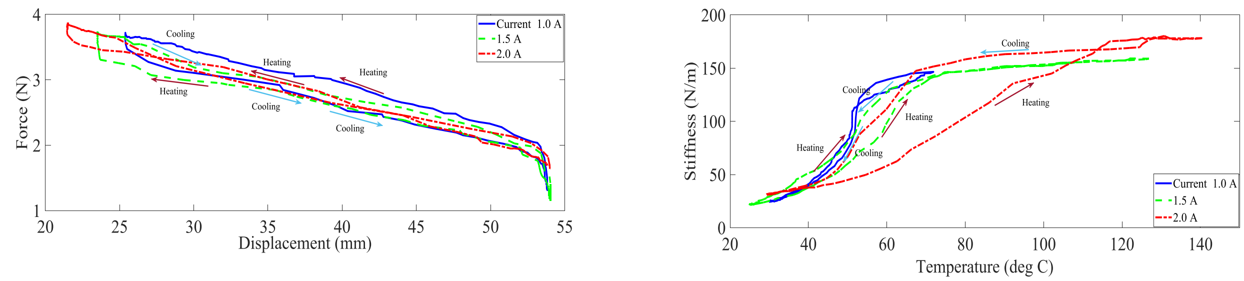

(a) (b)

Fig. 15 (a) Actuation characteristics of SMA spring at 10 mHz with different activation currents for Force to Displacement and (b) Actuation characteristics of SMA spring at 10 mHz with different activation currents for Stiffness to Temperature

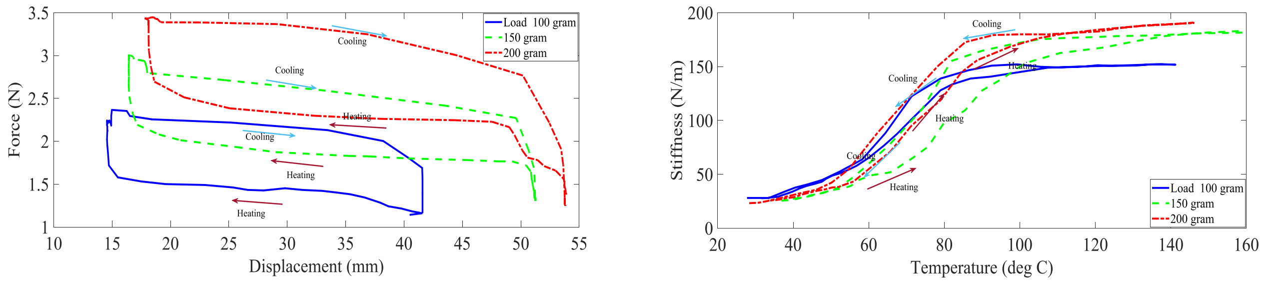

(a) (b)

Fig. 16 (a) Actuation characteristics of SMA spring at 10 mHz with different loads for Force to Displacement and (b) Actuation characteristics of SMA spring at 10 mHz with different loads for Stiffness to Temperature

displacement, force and stiffness, which are clearly seen in the Fig. 15.

It is observed that with increase in current, the temperature increases and in turn the displacement, force and stiffness too. The characteristics are presented corresponding to a driving frequency of 10 mHz. The effect of current on different properties of SMA is effectively/prominently seen at this frequency, since there is enough time for cooling and heating of the SMA spring.

Table 9 cites the minimum and maximum numerical values of stiffness of SMA spring in its heating and cooling cycle corresponding to the current within the range of effective actuation. The phase transformation is prominently visible in the current range of 1.5 A to 2.0 A where higher change in stiffness is noted, in comparison with the activation current that nears the safe heating value. It is obvious that the stiffness change from minimum value to maximum value is increasing with increase in current value.

7.1.2 The effect of stress / load

Experimentation is carried out to investigate the effect of stress / load on the SMA spring, exclusively with the application of varying load i.e., in the absence of the bias spring. A sinusoidal driving voltage signal is given at an amplitude of 0.5 V and frequency of 10 mHz The force and displacement profiles are obtained with varying temperature under various constant stresses ranging from 100 g to 200 g, these values of load are closer to the pull force is considered in order to see the effect of stress prominently on the mechanical properties of SMA spring; corresponding curves are shown in Fig. 16. It is observed from these characteristics that the hysteresis gap increases while the maximum force increases with the increase of applied stress. Whereas in displacement - temperature curve, the hysteresis band decreases and magnitude of displacement increases with increase in load. Therefore, the nonlinearity is prominent in force and stiffness characteristics as a function of temperature, at different stresses. So, a compromise is to be made between the nonlinearity and load of the SMA spring while put to use. The hysteresis curves with bias spring under constant load show that, the hysteresis gap is not affected by the stress on the force and displacement, maximum displacement decreases and force increases with respect to applied stress.

From the Table 10 cited, the stiffness exhibits linear change but obviously within the effective range of actuation. The phase transformation is prominent for the load change between 100 g to 150 g, where larger change in stiffness is exhibited, in comparison with the 150 g to 200 g.

7.1.3 The effect of driving frequency

To investigate further the effect of frequency on stiffness and other mechanical properties, a sinusoidal voltage with different frequencies is applied to comparator circuit and then MOSFET amplify current and decide the ON time to activate the SMA spring based on pulse modulated input.

From Fig. 18, displacement, force and stiffness increases very little with increase in frequency but at the same time hysteresis band decreases. At any constant frequency, the ‘S’ shape or sigmoid shape curve is obtained. And at higher frequencies, at the end of phase transformation temperature the curves become smooth; this phenomenon is due to the slow heat transfer rate. The more effective heating and cooling methods can be used to enhance the heat transfer rate.

Also it is seen from Fig. 18 that, the hysteresis band decreases and slope increases with increase in frequency for displacement, force and stiffness. Table 12 cites and observes the increase in frequency increases, increases the stiffness slightly.

The curves of displacement, force and stiffness profile as a function of temperature present similar nonlinear saturated characteristics. All the hysteresis curves of SMA spring are sigmoid-like, but they mainly differ by the hysteresis gap, curve slope and in their magnitude (minimum and maximum value of stiffness). Change in stiffness is observed with temperature, stress and frequency; while the range of change is major / maximum with change in temperature and it is lesser with the change in frequency and stress.

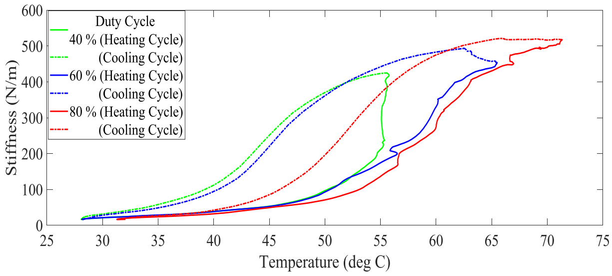

Fig. 17 Stiffness of SMA spring as a function of temperature at 2 A, 20 mHz, 56 MPa pre-stress at different duty cycles

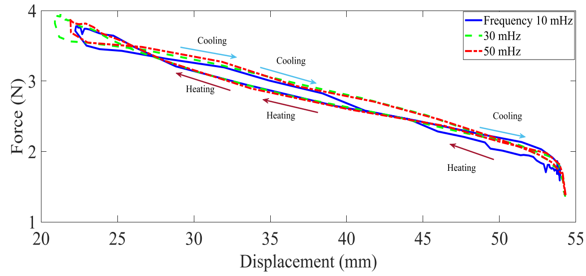

(a)

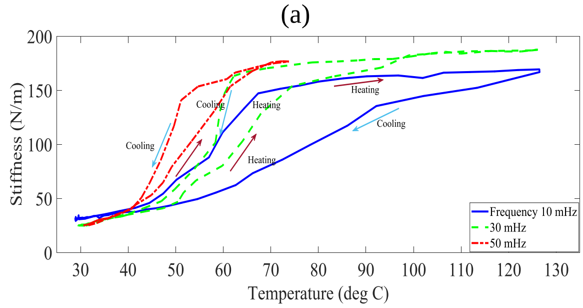

(b)

Fig. 18 (a)Actuation characteristics of SMA spring at 2 A with different frequencies for Force to Displacement (b)Actuation characteristics of SMA spring at 2 A with different frequencies for Stiffness to Temperature

7.1.4 The effect of duty cycle

The effect of duty cycle on stiffness is further investigated at 2 A, 20 mHz and 56 MPa pre-stress. From Fig. 17 correspondingly in Table 11, it is observed that stiffness increases consistently with increase in duty cycle but at the same time hysteresis band decreases. At any constant PWM frequency, the ‘S’ shape or sigmoid shape curve is obtained. And at higher duty cycle, at the end of phase transformation temperature the curves become smooth; this phenomenon is due to the slow heat transfer rate, more effective heating and cooling methods can be used to enhance the heat transfer rate.

Also it is seen that, the hysteresis band and slope of stiffness decreases with increase in duty cycle. The curves of stiffness profile as a function of temperature present similar nonlinear saturated characteristics. All the hysteresis curves of SMA spring are sigmoid-like, but they mainly differ by the hysteresis gap, curve slope and in their

Table 11 Effect of duty cycle on temperature and stiffness for 2 A current

Properties / Duty Cycle (%)	Temperature (°C)		Stiffness (N/m)	
	Minimum	Maximum	Minimum	Maximum
40	28.06	55.46	16.80	235.46
60	28.06	65.55	16.96	495.68
80	31.28	71.38	16.30	519.28

Table 12 Effect of frequency on temperature and stiffness at 2 A activation current

Properties / Frequency (mHz)	Temperature (°C)		Stiffness (N/m)	
	Minimum	Maximum		Minimum
10	29.16	126.81	10	29.16
30	29.40	126.13	30	29.40
50	31.00	73.80	50	31.00

magnitude (minimum and maximum value of stiffness). The duty cycle effects on the hysteresis of stiffness profile, thereby it can be changed to control or reduce the hysteresis gap. Indirectly duty cycle gives the information on heating speed and the highest temperature that the SMA can withstand. Also to produce the reproducible stiffness characteristics of SMA spring, understanding the hysteresis gap is a prerequisite (Wang *et al.* 2012).

7.2 Dynamic mechanical thermal analysis of the SMA spring

The Dynamic Mechanical Thermal Analysis (DMTA) is to be performed in order to verify the influence of excitation frequency, stress and temperature on the storage modulus (stiffness). The DMTA (Make Anton Paar) result of the SMA spring gives the idea about the temperature at which the mechanical properties start to stabilize. The difference in heat supplied and heat dissipated during heating becomes insignificant when heating rate approaches to zero. This observation is very important for practical applications that involve dynamical loads or mechanical vibrations. The storage modulus of the SMA spring for temperature sweep at different frequencies is presented in Fig. 19.

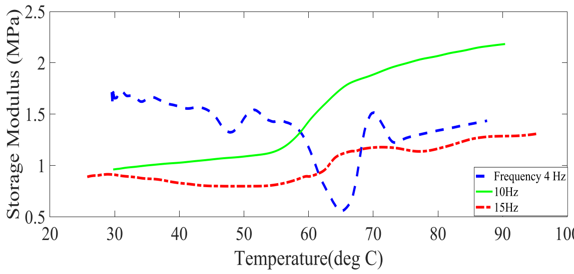

Fig. 19 The storage modulus of the SMA spring for temperature sweep at different frequencies

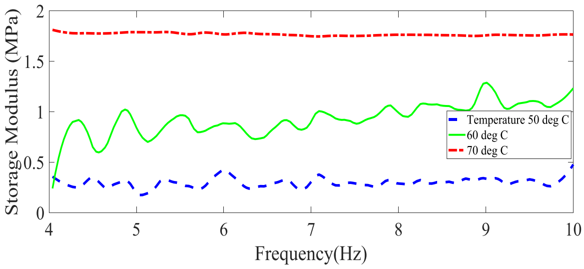

Fig. 20 The storage modulus of the SMA spring for frequency sweep at different temperatures

The behaviour of elastic modulus as a function of frequency shows small variations both for the martensitic and austenitic stable states, as shown in Fig. 20. Also the DMTA technique is used to measure the phase transition temperatures of SMA; which are difficult to be detected by the traditional methods, but DMTA gives quick and reliable results.

7.3 Cyclic loading effect

Ideally, SMA should completely recover its original shape, but practically after every loading cycle, a small residual strain is observed. During cyclic loading (thermal or mechanical), the partial recovery of inelastic strain increases until it saturates, after which the response remains stable. By training the SMA before deploying for an application, the inelastic strain can be reduced/removed. The goal of cyclic loading is eventual stability of the response of SMA as (He and Toi 013).

The effect of cyclic loading on the stiffness response of SMA spring intended for use as an actuator is determined by subjecting it to multiple transformation cycles under constant load, often called training. Here the test is performed at 150 g. Fig. 21 depicts the cyclic loading effect for 12 cycles; the initial displacement and stiffness response of SMA evolves with each cycle and, it eventually stabilizes (Lagoudas 2008).

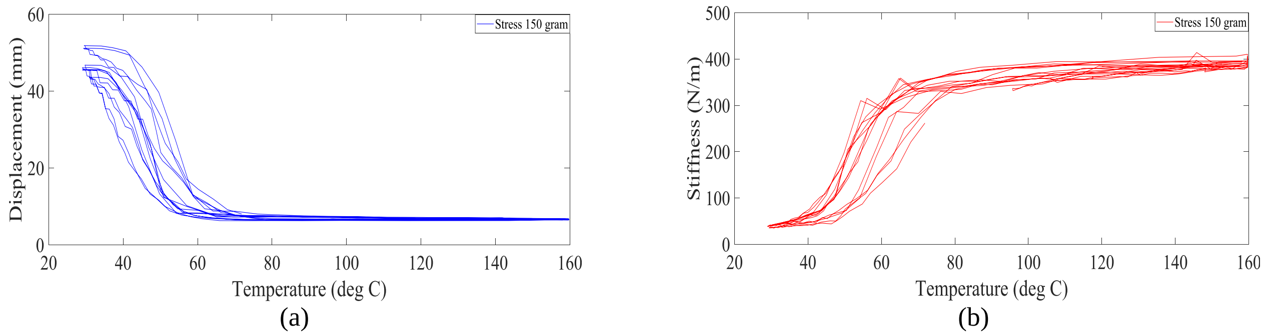

Fig. 21 Isobaric thermal cycling of SMA spring at constant stress for 150 g at 2 A (a) Displacement and (b) Stiffness

8. Conclusions

This study contributes betterment by modifying the sigmoid model of the nonlinear stiffness of SMA spring, which is an important phenomenon and viable control parameter. The kinetics of phase transformation of SMA spring is described and related through the complex and changeful stiffness with respect to temperature by a different mathematical model based on sigmoid function.

This article deeply explores the hysteresis characteristics between stiffness and temperature from the information of a series of experiments conducted under different conditions that affect the kinetics of phase transformation. These characteristics demonstrate the significance of the factors of SMA spring (frequency of excitation, stress/load and its temperature) and its effect on the spring rate. The set of parameters required to describe the proposed model is obtained by nonlinear least square / regression method. A set of experiments are conducted under different conditions that gives a correlation factor of 0.95 between the experimental response and the model response i.e., the function of the stiffness of SMA spring estimated by the proposed mathematical model shows good agreement with that obtained experimentally. The relevance of the modified sigmoid function based stiffness model of SMA coil spring is verified successfully by experimentation. It is also validated that the stiffness of SMA spring at austenite phase is more than 5 to 6 times higher than in the martensitic phase. It is readily apparent that the stiffness of SMA spring can be controlled mechanically by the temperature, moreover electrically by the control of current and supply frequency. The SMA spring with controllable stiffness is to be employed in systems requiring variable stiffness actuation like in soft robotics and active vibration isolation system (Enemark *et al.* 2015) and (Dhanalakshmi *et al.* 2011). The proposed modification of stiffness hysteresis is more flexible and capable of closely tracking the experimental response, in comparison with the logistic curve and polynomial models.

Acknowledgments

The research described in this paper was not financially supported.

References

Hadi, A., Yousefi-Koma, A., Elahinia, M., Moghaddam, M.M. and Ghazavi, A. (2010), "A shape memory alloy spring-based actuator with stiffness and position controllability", *J. Syst. Control Eng. Proc. I Mech E*, **225** Part I. https://doi.org/10.1177/2041304110394570.

Liang, C. and Rogers, C.A. (1997), "Design of shape memory alloy springs with applications in vibration control", *J. Intel. Mat. Syst. Str.*, **8**, 314-322. https://doi.org/10.1177/1045389X9700800404.

Dhanalakshmi, K., Umapathy, M., Ezhilarasi, D. and Bandyopadhya, B. (2011), "Design and implementation of fast output sampling feedback control for shape memory alloy actuated structures", *Smart Struct. Syst.*, **8**(4), 367-384. http://dx.doi.org/10.12989/sss.2011.8.4.367.

Kardan, I., Abiri, T., Kabganian, M. and Vahabi, M. (2013), "Modeling of shape memory alloy springs using a neural network", *J. Theor. Appl.Mech*., **51** (3), 711-718.

Zhang, J., Yin, Y. and Zhu, J. (2013), "Sigmoid – based hysteresis modeling and high speed tracking control of SMA –artificial muscle", *Sensor. Actuat. A - Phys.*, **201**, 264-273. https://doi.org/10.1016/j.sna.2013.07.036.

He, J. and Toi, Y. (2013), "Improved constitutive modeling for phase transformation of shape memory alloys", *J. Solid Mech. Mater. Eng.*, **7**(1), 11-26. https://doi.org/10.1299/jmmp.7.11.

Kumon, M., Mizumoto, I. and Iwai, Z. (2007), "Shape memory alloy actuator with simple adaptive control", *IEEE* 0-7695-2882-1/07.

Kciuk, M., Chwastek, K., Kluszczynski, K. and Szczyglowski, J. (2016), "A study on hysteresis behaviour of SMA linear actuators based on unipolar sigmoid hyperbolic tangent functions", *Sensor. Actuat. A - Phys.*, **243**, 52-58. https://doi.org/10.1016/j.sna.2016.02.012.

Cortez-Vega, R., Chairez, I., Luviano-Juarez, A. and Feliu-Batlle, V. (2018), "A hybrid dynamic model of shape memory alloy spring actuators", *Measurement***,** **114,** 340-353. https://doi.org/10.1016/j.measurement.2017.08.041.

Holanda, S.A., Silva, A.A., de Araujo, C.J. and de Aquino, A.S. (2014), "Study of the complex stiffness of a vibratory mechanical system with shape memory alloy coil spring actuator", *Shock Vib.*, Article ID 162781, 11 pages. http://dx.doi.org/10.1155/2014/162781.

Wolf, S., Grioli, G., Eiberger, O., Friedl, S., Grebenstein, M. and Carloni, R. (2016), "Variable stiffness actuators: review on design and components", *IEEE/ASME T. Mechatron*., **21**(5), 2418-2430. DOI: 10.1109/TMECH.2015.2501019.

Enemark, S., Savi, M.A. and Santos, I.F. (2015), "Experimental analysis of dynamical systems and involving shape memory alloys", *Smart Struct. Syst.*, **15**(6), 1521-1542. http://dx.doi.org/10.12989/sss.2015.15.6.1521.

Wang, T.M., Shi, Z.Y., Liu, D., Ma, C. and Zhang, Z.H. (2012), "An accurately controlled antagonistic shape memory alloy actuator with self-sensing", Sensors *MDPI Publications*, **12**(6), 7682-7700. https://doi.org/10.3390/s120607682.

Raczka, W., Konieczny, J. and Sibielak, M. (2011), "Mathematical model of a shape memory alloy spring intended for vibration reduction systems", *Trans. Tech. Publications*, **177**, 65-75. https://doi.org/10.4028/www.scientific.net/SSP.177.65.

Lagoudas, D.C. (2008), Editor, Shape Memory Alloys, Modeling and Engineering Applications, *Springer Science + Business Media, LLC.*

Sul, B.B. and Dhanalakshmi, K. (2017), "Sigmoid based force modeling and shape recovery characteristics of SMA spring actuator", *Proceedings of the 14th IEEE International Conference INDICON*, 15th -17th December 2017, IIT Roorkee, India.

Ikuta, K. (1990), "Micro/miniature shape memory alloy actuator", *Proceedings of the IEEE International Conference on Robotics and Automation*, 2156-2161.

Da Silva, N.J., Grassi, E.N.D., de Brito Simoes, J. and de Araujo, C.J. (2009), "Dynamic mechanical analysis of a NiTi shape memory alloy: An experimental study", *Proceedings of the COBEM 2009*, Gramado, RS, Brazil.

Bendame, M. (2010), "Mathematical modeling and control of nonlinear oscillators with shape memory alloys", *M. S. Theses, Wilfrid Laurier University.*

Van Ham, R., Sugar, T.G., Vanderborght, B., Hollander, K.W. and Lefeber, D. (2009), "Compliant actuator design", *IEEE Robotics and Automation Magazine*, 81-94.

www.sciencebuddies.com; Ben Finio, Ph.D.

HJ